

Optimization and reliability of multi-inversion time pseudo-continuous arterial spin labeling during rest and stimulus-induced functional task activation

Journal:	<i>Journal of Cerebral Blood Flow and Metabolism</i>
Manuscript ID:	JCBFM-0202-14-ORIG
Manuscript Type:	Original Articles
Date Submitted by the Author:	28-Apr-2014
Complete List of Authors:	Mezue, Melvin; FMRIB Centre, Nuffield Department of Clinical Neurosciences, University of Oxford Segerdahl, Andrew; FMRIB Centre, Nuffield Department of Clinical Neurosciences, University of Oxford Okell, Thomas; FMRIB Centre, Nuffield Department of Clinical Neurosciences, University of Oxford Chappell, Michael; University of Oxford, Institute of Biomedical Engineering; FMRIB Centre, Nuffield Department of Clinical Neurosciences, University of Oxford Kelly, Michael; FMRIB Centre, Nuffield Department of Clinical Neurosciences, University of Oxford Tracey, Irene; FMRIB Centre, Nuffield Department of Clinical Neurosciences, University of Oxford
Keywords:	arterial spin labelling, Brain Imaging, Cerebral blood flow measurement, Functional MRI (fMRI), Kinetic modelling, Physiology

Optimization and reliability of multi-inversion time pseudo-continuous arterial spin labeling during rest and stimulus-induced functional task activation

Melvin Mezue, DPhil ^{1*}§, Andrew R. Segerdahl, DPhil ^{1*}, Thomas W. Okell, DPhil¹, Michael A. Chappell, DPhil ^{1,2}, Michael E. Kelly, DPhil ¹, Irene Tracey, DPhil ¹

¹ Oxford Centre for Functional Magnetic Resonance Imaging of the Brain (FMRIB), Nuffield Department of Clinical Neurosciences, University of Oxford, Oxford, UK

² Department of Engineering, Institute of Biomedical Engineering, University of Oxford, Oxford, UK

* These authors contributed equally to this work

§ To whom correspondence should be addressed:

Dr Melvin Mezue
Centre for Functional Magnetic Resonance Imaging of the Brain (FMRIB)
John Radcliffe Hospital
Headington
Oxford, OX3 9DU
United Kingdom

Tel: +44 (0) 1865 234543
Fax: +44 (0) 1865 222717
Email: melvin.mezue@ndcn.ox.ac.uk

Running Head: Optimization of multi-TI pCASL during rest & task

ABSTRACT

Arterial spin labeling (ASL) sequences that incorporate multiple inversion times (TI) allow estimation of when arterial blood signal arrives within a region of interest. Sequences that account for such variability may improve the reliability of ASL and therefore make the technique well suited for future clinical and experimental investigations of cerebral perfusion. This study assessed the within- and between-session reproducibility of an optimised pseudo-continuous ASL fMRI sequence that incorporates multiple inversion times (multi-TI pCASL). Healthy subjects underwent 4 identical scans separated by 30 minutes, one week and one month using multi-TI pCASL to image absolute perfusion (cerebral blood flow [CBF] and arterial arrival time [AAT]) during both rest and a visual-cued motor task. We show good test-retest reliability, with strong consistency across subjects and sessions during rest (inter-session within-subject coefficient of variation: GM CBF = 6.44%; GM AAT = 2.20%). We also report high sensitivity and reproducibility during the functional task, where we show robust task-related decreases in AAT corresponding with regions of increased CBF. Importantly, these results give insight into optimal TI selection for future investigations employing single-TI ASL to image different brain regions, and highlight the necessity of multi-TI ASL when imaging perfusion in the whole brain.

KEYWORDS

ASL, brain imaging, cerebral blood flow measurement, fMRI, kinetic modelling, physiology

INTRODUCTION

An exciting experimental direction in the field of magnetic resonance imaging is towards non-invasive quantification (in absolute units) of physiological parameters such as cerebral blood flow (CBF), cerebral blood volume (CBV), and cerebral metabolic rate for oxygen (CMRO₂). MRI-based techniques offer the advantage of comparatively high spatial resolution without the use of ionising radiation or intravenous contrast agents.

Currently, measurements of CBV and CMRO₂ are possible but are largely hindered by such issues as poor signal-to-noise ratio (SNR), low temporal resolution and inadequate statistical modelling.^{1,2} However, recent advances in both scanner hardware and pulse-sequence design have greatly improved the utility of Arterial Spin Labeling (ASL); a technique that uses the magnetization of arterial blood water as an endogenous contrast agent for the quantification of CBF.^{3,4} ASL techniques are attractive to both clinical and experimental studies as they offer the ability to investigate long acting cognitive and physiological states (not possible with Blood Oxygen Level Dependent (BOLD)), and to complete multiple repeat scans (e.g. follow-up investigations, longitudinal designs, pharmacological trials) without cumulative risk to the subject. In particular, pseudo-continuous ASL (pCASL) provides high labeling efficiency and signal-to-noise ratio (SNR) without the need for custom hardware.⁵

ASL has been shown in resting functional studies to be reproducible and to reflect activation patterns similar to BOLD, although with potentially better specificity and co-localisation between subjects (due to less inter-subject variability).^{6,7} In addition, CBF-

1
2
3 based measurements are more localised to the relevant parenchyma than the BOLD
4
5 effect.^{6,8} While the exact dynamic relationship between neural function and CBF is not
6
7 yet well known, considerable evidence suggests that imaging CBF alone offers a strong
8
9 correlate of brain function.^{9,10,11}
10
11

12
13
14 While it has been shown that ASL provides an effective tool for rapid and safe
15
16 estimation of blood flow in resting, task-related and pharmacological fMRI studies^{4,12,13};
17
18 only a handful of studies have investigated how reliable these measures are and fewer
19
20 still have looked at ways to improve this. For example, continuous ASL (CASL)
21
22 techniques have been shown to be accurate and highly reproducible within 1-hour¹⁴ and
23
24 7-week timeframes¹⁵. When compared to pulsed ASL (ASL) and CASL, pCASL is
25
26 shown to be the least variable.^{16,17,18} Longitudinal repeatability of pCASL has also been
27
28 validated for neuro-developmental studies in children.¹⁹
29
30
31
32
33
34
35

36
37 ASL sequences that incorporate multiple inversion times (TIs) allow estimation of when
38
39 blood signal arrives at the voxel of interest²⁰; a feature that is known to vary spatially
40
41 according to position within the vascular tree. Sequences that account for this variability
42
43 in arterial arrival time (AAT) can be used to improve the reliability of ASL; thereby
44
45 supporting its use to image more complex conditions where cerebral perfusion may be
46
47 undermined by a particular pathology.²¹ Recent work supports this by showing that: i) it
48
49 is possible to account for heterogeneity in AAT by incorporating multiple TIs^{22,23}; ii)
50
51 acquisition of multiple TIs improves the accuracy of CBF quantification by facilitating the
52
53 removal of the macro-vascular component of the ASL signal.²⁴
54
55
56
57
58
59
60

At present, no study has assessed the within- and between-session reproducibility of multi-TI pCASL. Given the potential relevance of this technique for longitudinal studies and assessment of drug efficacy or long acting cognitive and physiological states, we suggest this is an important initial investigation of the method with a view towards improving its experimental and clinical utility.

The primary aim of this study was to assess whether a multi-TI pCASL sequence is a reliable method for imaging absolute perfusion across a whole brain volume during rest versus a visual-cued motor task. The secondary aim of this study was to measure the across subject and across session variability in both whole brain grey matter and a number of key brain regions.

MATERIALS AND METHODS

Subjects

Variability of multi-TI pCASL was assessed at three imaging sessions completed on 8 healthy subjects (6 male, 2 female age [mean ± s.e.m]= 28.3 ± 2.5) at the FMRIB Centre, University of Oxford, John Radcliffe Hospital, Headington, UK. Subjects were asked to abstain from caffeine for 6 hours prior to each session. In addition to routine screening for MRI contraindications, subjects were also screened to exclude any

1
2
3 cerebrovascular disease, neurological/psychiatric disease, and use of medication that
4 could interact with blood flow. All procedures described were performed under an
5 agreed technical development protocol approved by the Oxford University Clinical Trials
6 and Research Governance office, in accordance with International Electrotechnical
7 Commission and United Kingdom Health Protection Agency guidelines.
8
9
10
11
12
13
14
15
16
17
18
19
20
21

22 ***Study design***

23
24 Subjects were scanned on three separate occasions, separated by one week and one
25 month, respectively. Session 1 consisted of two repeat runs of the experimental
26 protocol, separated by a 30-minute rest period; while session 2 and 3 had only a single
27 run (Figure 1). The protocol consisted of a 6-minute resting CBF scan followed by a 6-
28 minute OFF/ON visual-cued motor task (8Hz flashing checkerboard with combined
29 finger-tapping)- alternating 1 minute ON and 1 minute OFF. The majority of scans took
30 place between 8am and 12pm to minimise diurnal variation, which can affect CBF
31 values.²⁵
32
33
34
35
36
37
38
39
40
41
42
43
44
45
46
47

48 ***MR data acquisition***

49
50 All subjects were scanned using a Siemens 3T Verio whole-body MR scanner
51 (Erlangen, Germany) equipped with a 32-channel head coil and a body coil. We used a
52 modified pCASL pulse sequence⁵ for image acquisition. A time-of-flight MR angiography
53
54
55
56
57
58
59
60

neck scan was acquired approximately 8cm below the circle of Willis to visualise the brain's feeding arteries. The labeling plane was aligned perpendicular to the ascending carotid and vertebral arteries. The location of the plane was normalised to a point between the curvatures of the vertebral arteries, where all feeding arteries ran parallel in a transverse plane. B0 shimming²⁶ was performed over the imaging region and the labeling plane to minimise off-resonance effects.

We used a pCASL acquisition sequence with background suppression as described previously.²⁷ Images were acquired in separate consecutive blocks, each composing 6 different post-labeling delays: 0.25, 0.5, 0.75, 1, 1.25, 1.5 (seconds). A labeling duration of 1.4 seconds was used. The selected range of inversion times encompasses those that are commonly used in the literature for both single and multi-TI ASL approaches, as was recently validated for use in human subjects to adequately model kinetic curves for all voxels across a whole brain volume.²⁷ Other imaging parameters were: single shot EPI, TR = 4s, TE = 13ms, Partial Fourier = 6/8^{ths}, FOV = 220x220, matrix = 64x64, 24 ascending slices, slice thickness = 4.95mm, slice acquisition time = 45.2 ms. For each scan, 96 volumes (control and tag) were acquired, corresponding to 6.4 minutes of scanning. Data was analysed as 8 separate epochs where each epoch represented a full set of control/tag images for all 6 Tis.

A reference calibration image (no labeling or background suppression, TR=6s, all other parameters identical to pCASL scan) was also collected to enable the estimation of the equilibrium magnetisation of blood. A second calibration image of the same prescription was collected using the body coil for signal detection. This body coil calibration scan

was used to correct the PCASL data for the uneven sensitivity profile of the 32-channel head coil.¹⁸ A T1-weighted structural image was acquired for tissue segmentation and registration purposes. We additionally acquire a phase contrast angiography image (TR=72.9ms, TE=4.82ms, FOV=240x240, matrix=128x128, slice thickness=5mm, flip angle=15 degrees, velocity encoding=100cm/s) in the same position as the labeling plane to assess blood flow velocity and inversion efficiency,²⁸ and corresponding B0 field map images to correct for EPI distortion effects.

Data Processing

FSL (FMRIB Software Library, Functional Magnetic Resonance Imaging of the Brain Centre, Department of Clinical Neurosciences, University of Oxford, Oxford, UK, <http://www.fmrib.ox.ac.uk>) and Matlab were used for offline data processing.

Pre-quantification processing

All raw ASL data collected from each subject were stripped of non-brain structures using BET²⁹; and motion corrected using MCFLIRT.³⁰ Pairwise subtraction of 'tag' and 'control' images was performed on the data to generate perfusion-weighted images.

Quantification of CBF

All related data processing steps essential for quantification of CBF including tissue segmentation, estimation of equilibrium magnetization of blood ($M0_b$) from the mean cerebrospinal fluid (CSF) magnetization ($M0_{csf}$) images, and generation of absolute CBF

in physiological units (ml blood/ 100g tissue/ 60 seconds) were completed using FSL tools. For a detailed explanation of the processing performed to obtain quantification of CBF, CBF uncertainty and arterial arrival time (AAT) from the PCASL data please refer to (ref. 27).

Briefly, quantification of absolute blood flow requires estimation of the equilibrium magnetization of arterial blood. To do this, we divided the head and body coil images to generate a coil sensitivity map. This map was then used to correct the reference image and the PCASL data before CBF quantification to correct for the uneven sensitivity profile of the 32-channel head coil. Additionally, a pairwise control minus tag subtraction was performed on the PCASL data to generate a perfusion image at each inversion time. The resultant voxel-wise concentration-time curves were fitted to the general kinetic model¹⁰ to estimate both CBF and AAT.

Perfusion parameters were quantified using multicomponent modelling with a Bayesian inference tool (BASIL) developed for this purpose (<http://fsl.fmrib.ox.ac.uk/fsl/fslwiki/BASIL>).^{24,31} BASIL outputs voxel-wise estimates of absolute CBF and AAT, as well as a corresponding voxel-wise variance map for each parameter. Importantly, these parameters were estimated for each epoch of data (defined as a full set of inversion times), thus generating a time series of absolute CBF and AAT from each acquisition. 8 such epochs were generated from each scan. Please refer to (refs. 24, 27, 31) for a full description of the variational Bayes approach implemented by BASIL to incorporate prior information about known physiological

parameters (e.g. TI, blood T1) and varying parameters (i.e. post-label delays) to improve CBF estimation.

Post-quantification processing

Resting data

The time-series of epochs generated for each scan was averaged using a mixed effects model, which accounted for the voxel-wise variance of the Bayesian fit. This generated a single CBF and AAT image for each scan, with a corresponding variance image. For comparisons, raw EPI images were registered first to each subject's structural image using BBR³², then non-linearly to the MNI standard brain using FNIRT.³³ Transformed quantified images were used for voxel-wise statistical comparisons described below.

Task data

The epochs were concatenated such that volumes alternated between a full rest block and a full visuomotor active block- i.e. for each 1 minute stimulation period, a single epoch of absolute CBF was generated. Specifically, the initial 12 seconds of each 60 second functional acquisition block was discarded to ensure a steady-state during each 48-second epoch acquisition. The resultant data timeseries (6 epochs- 3 rest and 3 task) were modelled using a GLM square design to generate a statistical map of brain regions responding to the visuomotor task. A significance map was generated with a cluster corrected Z threshold of 2.3 ($p < 0.05$). Statistical images were transformed to standard space for group comparisons. A mixed effects model (FLAME 1+2) was used

to assess group level effects. CBF values were extracted from grey matter (GM), and region-defined voxels for each subject and session.

Statistical analysis

Within and across subject variation was calculated using IBM SPSS Statistics, version 18 (IBM, Armonk, NY, USA). This was assessed for grey matter (GM), four major lobes (frontal, temporal, parietal, occipital) and a selection of brain regions bilaterally (insula cortex [INS], thalamus [THA], caudate [CAU] and putamen [PUT]) using masks generated from FAST³⁴, and the MNI Structural Atlas (thresholded at $p > 0.5$, binarised). These masks were transformed back into the image acquisition space for extraction of CBF and AAT values.

Repeatability of resting measures

We assess repeatability of resting physiological variables using three separate methods: evaluating within-subject coefficients of variation (wsCV) and intraclass correlations (ICC); analyses of variance (with pairwise t-tests) between the CBF values extracted from regions of interest; and voxel-wise comparisons between the different conditions in the framework of a general linear model. We calculated wsCV values from the ratio of the standard deviation of the difference between the repeated measures, to the mean of the repeated measures.³⁵ A smaller wsCV number represents better reproducibility. Within- and across-session variation between subjects was quantified for CBF and AAT by calculating session-paired wsCV and ICC. We assessed intra-subject variation by calculating across-session wsCV using CBF values from the three sessions

for each subject. These were averaged for all subjects to give a mean intra-subject wsCV. ICC measures the contribution of between subject variances to total variance. We calculated two-way mixed single measures of ICC in SPSS for absolute agreement between measures as described previously³⁶:

$$ICC_{(3,1)} = (BMS - EMS) / (BMS + (k - 1) * EMS) \quad (1)$$

[where BMS is between targets mean square, EMS is error mean square and k is number of repeat sessions]

ICC values range from 0-1: we designate ICC values <0.4 as poor, 0.4-0.59 as fair, 0.60-0.74 as good, and >0.75 as excellent.³⁷ These denotations do not account for confidence intervals so must be interpreted cautiously.

To investigate type I error inherent in the technique, we perform repeated-measures analyses of variance and paired comparisons (student paired t-tests) between session-wise and run-wise regional CBF values using SPSS. We used a 0.05 σ threshold as evidence of good specificity of the technique. To assess differences between whole-brain CBF and AAT values, we performed a voxel-wise GLM analysis in a higher level FEAT analysis (www.fsl.ox.ac.uk/feat).

Repeatability of task measures

Type II error was assessed across all scan sessions by evaluating CBF percentage change between task and rest blocks in an *a priori* defined anatomical mask for the

primary visual cortex. We used a value of $\beta < 0.2$ as evidence of good sensitivity.

We assessed repeatability of task measures by performing analyses of variance and paired t-tests between run-wise and session-wise absolute CBF changes (ΔCBF) and AAT changes (ΔAAT) from each ROI. Anatomical ROIs were derived from the Harvard-Oxford Atlas in FSLTools (thresholded at $p > 0.5$ and binarised). Functional masks for the visual and motor cortices were defined by 5-mm spheres centred on the peak active voxel within the anatomical masks for each region. Finally we test session-wise and task-wise reproducibility of the CBF change by performing a whole-brain voxel-wise analysis of variance between the sessions using FEAT.

Optimization of inversion time selection

To assess the utility of our selection of inversion times in the context of single TI experiments, we calculate an optimization metric (γ) that reflects how well CBF measures are observed across the whole brain.

For single-TI studies, in order for the measured signal to reflect CBF, the AAT must be shorter than the post-labeling delay (PLD)- i.e. tagged blood must arrive at the region of interest before imaging. Because a fixed calculation is used to fit the peak magnetization of arterial signal within a given voxel in multi-TI analysis, we can assess the ability of a given TI to accurately estimate CBF by comparing the estimated AAT to the delay time between tagging and imaging (PLD + slice acquisition time; slice dt):

$$\gamma = AAT - (PLD + [z * slice\ dt]) \quad (2)$$

[where AAT= arterial arrival time; PLD post labeling delay; z=number of slice acquired in ascending order; slice dt= acquisition time per slice]

Regions where $\gamma > 0$ indicates when slice acquisition begins before the AAT; while $\gamma < 0$ reflects areas within which acquisition occurs after AAT. We assume that the most optimized setting for SNR would be when the time it takes for arterial signal to arrive at a voxel is equal to the PLD (i.e. $\gamma = 0$). For CBF signal, the most optimised setting is where $\gamma \leq 0$ as this ensures adequate blood arrival. Calculation of the optimization metric (γ) is useful as it informs selection of inversion times for whole-brain multi-TI studies. It also can be used to select an appropriate PLD for use in a single-TI ASL experiments to maximise signal in a given brain region. To illustrate this point, we plotted histograms for three key ROIs to visualise the range of γ values for each TI used in the study (Supplementary Figure 3 a-c).

RESULTS

Before reporting the absolute perfusion data, we checked that the $M0_b$ values generated from the absolute quantification processing steps were reliable. Because the $M0_b$ is an

essential variable from which the relative perfusion data is scaled into physiological units, it is essential for this to be reliable for each subject at each scan session. We report that the wsCV for $M0_b$ during the week and month repeat scans were 3.45% and 2.42%, respectively. The wsCV for all scan sessions was 2.77%.

Repeatability of resting physiological measures

Average CBF and AAT values from all ROIs are shown in Supplementary Tables 1 and 2. We see heterogeneity in CBF and AAT between subjects and between regions. Bland Altman plots (with 95% confidence intervals) show mean CBF versus the difference in CBF values in selected ROIs (Figure 2). Intra- and inter-subject repeatability measures (wsCV and ICC) are shown for CBF and for ATT in Tables 1 and 2, respectively. There is evidence of good to excellent reliability ($ICC > 0.6$) and moderate to high reproducibility ($wsCV < 10\%$) for most measures.

Repeatability measures are shown to be stronger with shorter inter-scan intervals. For example, wscV for GM CBF ranged from 3.37% within session to 9.95% for a month repeat scan while ICC ranged from 0.914 to 0.181, respectively. . CBF and AAT reliability measures also showed heterogeneity between different ROIs: for CBF, white matter (ICC: 0-0.668) and the insula cortex (ICC: 0.06-0.67) showed the lowest reliability while the thalamus (wsCV 9.2-13.53%) and occipital lobe (6.79-13.46%) showed the least reproducibility. AAT repeatability analyses showed uniformly lower wsCV values ($< 5\%$) in comparison to CBF, indicating better reproducibility.

In 1x3 ANOVAs testing the effect of session on extracted CBF and AAT values, there was no significant difference between any of the tested regions ($p>0.05$). There were no significant changes in AAT values between runs 1 and 2 in session 1 for all ROIs tested. However, we report an average CBF decrease of 10.5% in an anatomical mask of the thalamus between runs 1 and 2 (*corrected* $p=0.045$). No other brain regions tested show within-session CBF changes.

In a voxel-wise ANOVA comparison of sessions, there was no significant effect of session on voxel-wise CBF across the whole brain (mixed effects, cluster corrected, $Z=2.3$).

Repeatability of CBF response to active task

Figure 3 shows brain regions that respond significantly (increased CBF) to the visual-cued motor task for all runs. For all task ON blocks, in all sessions, we report the power ($1-\beta$; ON vs. OFF) for signal change in the anatomical V1 as greater than 0.9. For all functional masks, the power is approximately equal to 1. The mean task-induced % changes in CBF during ON vs. OFF blocks for each run and session are shown in Table 3. We also report significant decreases ($p<0.05$) in AAT in the anatomical V1 and in functional masks derived from the regions of significant CBF increases during task-induced activation within primary visual and motor cortices. These changes in AAT are shown in Supplementary Table 3.

Comparisons of extracted Δ CBF and Δ AAT from both within and across sessions showed no significant differences in either the anatomical or functional ROIs (CBF,

within-session Student T-test: $p=0.75$; between-session ANOVA: $p=0.90$, $F=0.107$). Similarly, a FEAT analysis revealed no significant differences in extent of CBF changes with task ON vs OFF blocks either within or across sessions (voxel-wise mixed effects analysis; $z>2.3$; $p<0.05$, cluster corrected).

Optimization of inversion time selection

Figure 4 shows inversion time benefit values (γ) mapped onto a standard brain for each individual inversion time selected. Most cortical regions have been adequately perfused by labelled blood with a PLD of 1 s, although many inferior regions are maximally perfused subsequent to this. Regions where $\gamma>0$ indicates when slice acquisition begins before the AAT (red); while $\gamma<0$ reflects areas within which acquisition occurs after AAT (blue).

To interrogate this further, we plotted ROI-specific histograms of the percentage of voxels observed to have $\gamma<0$ for each PLD used in the paradigm (Figure 6a-c). Regional masks were generated from the Juelich, MNI, and Harvard-Oxford Subcortical Atlases respectively ($p>0.5$). We designate inversion times where most voxels have values close to zero as optimal for both SNR and CNR. For single-TI studies using such a protocol, we therefore suggest the optimal PLD selection to be 0.5 for the motor cortex, 0.25 for the insula and 1 for the amygdala (Supplementary Figure 3). For multi-TI experiments targeting these regions, the range of PLDs should be clustered around these optimal values.

DISCUSSION

The results from this study show that the multi-TI pCASL approach has high test-retest reliability as the data reveal strong consistency across subjects and sessions for key perfusion outcome measures (AAT and CBF). Specifically, we report low variation coefficients, high interclass correlation coefficients and good effect specificity in standard GLM-based analyses of the ASL data. Additionally, we successfully validated the reliability of this newly developed tool for assessment of functional tasks; a novel feature which has not been investigated for pCASL imaging to our knowledge. Importantly, the results of this study give insight into optimal TI sampling schedules across different brain regions for healthy populations and suggests the importance of multi-TI pCASL for whole brain acquisitions as the single TI approach will only be optimal for imaging select regions. Furthermore, in older subjects or patient groups where blood flow may be more variable, the flexibility of the multi-TI approach will be desirable.

Resting perfusion measures are reliable and reproducible

Assessment of CBF across the whole brain shows both the wsCV(%) and the ICC measures to be reliably consistent across session repeats on the same day, a week and a month later. However, these measures show slight depreciation in exact reproducibility as the duration between scan sessions increases.

Specifically, the data show good to excellent longitudinal reproducibility across most brain regions for both CBF (wsCV= 5.33%, ICC= 0.711 for grey matter over 1 week) and AAT (wsCV=3.25%, ICC= 0.526 for grey matter over 1 week). In general, within subject repeatability measures less than 20% are suggested to be in the normal range for ASL studies.¹⁷ Previous reports show moderate to good longitudinal reproducibility (ICC= 0.65, wsCV= 14% for grey matter) for pCASL over a 2-4 week period in a paediatric cohort ¹⁹; while other studies of week-repeat comparisons report whole brain/regional wsCV to be between 8-14%.^{14,16} The data we report here are consistently within this range or show improved reliability (i.e. values are lower) when compared to previous investigations of the same session comparisons.

We find no differences in session-wise ANOVAs for extracted data and voxel-wise GLM analyses, suggesting high specificity for the technique across 1-week and 1-month comparisons. Interestingly, we show that in a within-session comparison where both runs are separated by 30 minutes, there is a significant decrease in thalamic CBF (Supplementary Figure 1). The thalamus is a key relay centre and is an important shared anatomical substrate for both arousal and attentional processes.³⁸ Given that subjects were lying in the scanner without attending to any task in the intervening period, we suggest that this reduction in thalamic CBF may reflect decreased attentional processing between the early and late scans. This is supported by a lack of significant differences between corresponding CBF responses to the functional task, where attention/arousal is better matched.

These data support the conclusion that the mean variation intrinsic to the technique is lower than what is associated with general physiology for within and between session comparisons. Therefore, we conclude that the technique is reliable for use in longitudinal studies over similar time-frames; with the caveat that it is optimally suited for within session or more short-term crossover studies.

Reliability and sensitivity to functional changes in physiology

We find that the multi-TI pCASL approach is highly sensitive (power consistently >0.9 in an *a priori* defined anatomical mask) to functional CBF changes in a salient visual-cued motor task (Figure 3). Importantly, analysis of variance associated with the extracted CBF values and voxel-wise cluster corrected statistics maps generated in FEAT reveal no significant run-wise or session-wise differences between functional CBF responses to the task. This suggests that the sensitivity of the technique is reliable and that it can be used to test long (>1 minute) activation states in the context of multiple study visits. To our knowledge, this is the first report of ASL reproducibility of stimulus-induced functional activation. Additionally, we report a significant decrease in AAT within regions that show a significant increase in CBF during the visual-cued functional task (Supplementary Table 3). While the current study is not designed to interrogate the neurovascular dynamics linked to tonic stimulation, these data show for the first time that the multi-TI pCASL approach is capable of reliably quantifying neurovascular-related signal changes fundamental to fMRI analysis and interpretation; and may facilitate future work in this direction that was previously limited by the nontrivial limitations of other commonly used imaging approaches.

Benefit of multi-TI approach to increase reliability

A recent study⁵ highlights the importance of multiple PLD acquisitions to help account for AAT heterogeneity between subjects and brain regions. Although the acquisition length of the paradigm used in the current study is comparable to similar ASL investigations employing single TI pCASL sequences, the analysis of the multi TI data yields time courses constituent of only 8 epochs of absolute perfusion data (i.e. the multi TI approach necessitates far less averaging of ASL data over time). Considering this in the context of the subject- and region-wise AAT variability data discussed above, the multi TI approach may improve the reliability and specificity of pCASL to estimate absolute perfusion by accounting for bolus arrival time variability across the whole brain volume. A comparison between single-TI and multi-TI acquisitions may further clarify these benefits.

Interestingly, we also show that both CBF and AAT reliability decrease as repeat interval time increases. As was proposed previously¹⁵, this likely reflects physiological variability over long time periods rather than increases in measurement error. ICC values also show more variability than wsCV in this respect. It should be noted that while wsCV normalises to the mean and so is unbiased, ICC depends on the ratio of within- to between-subject variance; a feature that can vary significantly between sessions. Nonetheless, we report ICC values that are comparable or improved when considered in the context of previously published pCASL reproducibility studies.^{19,22}

Optimising inversion time selection for ROIs

Interestingly, when interrogating ASL reproducibility at the level of specific ROIs, this effect is slightly more complex. Specifically, both CBF and AAT are reliably reproducible across subjects and, like the whole brain volume data, are most reliably reproducible across runs of the experiment within the same scan session. As above, when the delay between repeat scans increases, the reliability decreases; though the extent of this depreciation is ROI-dependent. In general, smaller, more subcortical regions appear to show considerably reduced reliability when viewing the month-repeat session comparisons (e.g. amygdala wsCV = 15.0). However, regions like the hippocampus are observed to be more reliably reproducible (e.g. wsCV = 10.1) and approximate what we see within cortical lying structures. The exact cause for this is likely to be due to physiological variables such as cerebrospinal fluid (CSF) and related motion confounds associated with cardiac output and respiration; strong undermining sources of variance that are not easily accounted for with standard fMRI analysis tools currently available. Future studies looking at imaging these structures with ASL will likely benefit by increasing the population size being scanned while modeling individual subject's physiology (e.g. heart rate, breathing rate, etc) to improve the overall quality of perfusion images collected. It may also be important to tailor the inversion time selection to the brain region being investigated.

To explore this possibility, we analysed the voxel-wise inversion time efficiency at each chosen PLD across a number of ROIs. A region is said to have an SNR-optimal inversion time selection if its AAT corresponds closely with the time of imaging ($\gamma = \sim 0$)

(Figures 4 & 5). For single TI studies, $\gamma < 0$ is needed to ensure adequate blood arrival before image acquisition. It should be noted that the optimization values we report are specific to our sequence and protocol as they depend on variable scanner parameters (e.g. slice timing). We show that there is regional heterogeneity in efficiency across the brain (particularly in the superior-inferior domain) for different PLDs. However, most regions of the brain reach peak ASL signal within a 1-second PLD- this corroborates similar findings in healthy subjects using an adaptive sequential design (ASD) strategy that modifies the optimal sampling time regionally in real time.³⁹

These findings suggest that inversion time selection for single TI studies should be optimised depending on the region of interest. In the case of a whole-brain acquisition, a multi-TI approach may be better suited to account for regional heterogeneity. In the context of a functional experiment in a healthy cohort, arrival time decrease during regional activation (Supplementary Table 3), making a single TI approach suboptimal. In such studies, it may also be appropriate to narrow and centre the PLD range around 1 second, allowing better sampling of the kinetic curve or reduction of the number of PLDs to improve temporal resolution.

Limitations

As with any exploratory investigation of a novel imaging modality, there are a number of limitations we must address. Firstly, we tested a small cohort that were scanned multiple times using the same MRI scanner. The next step will be to repeat this type of investigation with a larger cohort of subjects scanned on different 3T scanners as was

done for single-TI pCASL sequences.^{17,40} Also, we used healthy volunteers from a similar age group. However, it is known that cerebral perfusion measured by ASL is influenced by age alongside a number of physiological variables.²⁵ It is important to optimise the multi-TI analysis tools to appropriately model these sources of variance either by modifying the labeling efficiency assumptions and/or the range of inversion times used. Currently, modelling subject-specific physiological variation into the calculation of absolute CBF remains difficult given the multi-TI Bayesian inference approach used. However, tools able to account for intra-subject variability in CO₂, blood pressure and cardiac cycle may account for variation in inversion efficiency (i.e. tagging of arterial blood)²⁸ to improve ASL reliability further. These enhancements may facilitate investigation of patient groups, especially those with cerebrovascular conditions and/or on medications likely to affect CBF and AAT as well as more complex experimental design paradigms currently outside the realm of the technique.

Conclusion

The results from this study show for the first time the utility of employing a multi-TI pCASL imaging approach to reliably image normal human brain function at rest and during a stimulus-evoked functional task. The key benefit of employing a multi-TI approach to ASL is that it allows noninvasive investigation of brain function beyond just relative changes in arterial signal. As the data described here show, the technique is able to reliably observe both arterial arrival time and CBF: outcome measures essential for improving our understanding of key features of brain physiology, function and related pathology. In addition, we show how assessment of these variables across ROIs

highlights a number of interesting perfusion features that vary with anatomical location. Preliminary analysis of some of these features suggests that future investigations able to further optimise TI selection based on anatomy may improve the across-session reliability of the technique for imaging subcortical structures. The data presented here show that this technique is not only robust and reliable but is also a novel alternative to more commonly applied ASL approaches because of the added experimental flexibility the multi-TI approach offers. We are confident this approach will provide a powerful tool for future functional studies of long activation states, clinical diagnostic approaches and novel drug development.

Supplementary information is available at the Journal of Cerebral Blood Flow & Metabolism website – www.nature.com/jcbfm

DISCLOSURE/CONFLICT OF INTEREST STATEMENT

The authors declare no conflict of interest.

REFERENCES

- 1) Uh J, Lewis-Amezcu K, Varghese R, Lu H. On the measurement of absolute cerebral blood volume (CBV) using vascular-space-occupancy (VASO) MRI. *Magn Reson Med* 2009; 61: 659-67.
- 2) Blockley N, Griffeth V, Buxton R. A general analysis of calibrated BOLD methodology for measuring CMRO₂ responses: Comparison of a new approach with existing methods. *Neuroimage* 2012; 60: 279-89.
- 3) Williams D, Detre J, Leigh J, Koretsky A. Magnetic resonance imaging of perfusion using spin inversion of arterial water. *PNAS* 1992; 89: 212-6.
- 4) Detre J, Wang J, Wang Z, Rao H. Arterial spin-labelled perfusion MRI in basic and clinical neuroscience. *Curr Opin Neurol* 2009; 22: 348-55.
- 5) Dai W, Garcia D, de Bazelaire C, Alsop D. Continuous flow-driven inversion for arterial spin labeling using pulsed radio frequency and gradient fields. *Magn Reson Med* 2008; 60: 1488-97.
- 6) Tjandra T, Brooks JC, Figueiredo P, Wise R, Matthews PM, Tracey I. Quantitative assessment of the reproducibility of functional activation measured with BOLD and MR perfusion imaging: implications for clinical trial design. *Neuroimage* 2005; 27: 393-401.
- 7) Raoult H, Petr J, Bannier E, Stamm A, Gauvrit JY, Barillot C, Ferre JC. Arterial spin labelling for motor activation mapping at 3T with a 32-channel coil: reproducibility and spatial accuracy in comparison with BOLD fMRI. *Neuroimage* 2011; 58:157-67.
- 8) Pfeuffer J, Adriany G, Shmuel A, Yacoub E, Van De Moortele PF, Hu X, Ugurbil K. Perfusion-based high-resolution functional imaging in the human brain at 7 Tesla. *Magn Reson Med* 2002; 47: 903-11.
- 9) Fox P & Raichle M. Focal physiological uncoupling of cerebral blood flow and oxidative metabolism during somatosensory stimulation in human subjects. *PNAS* 1986; 83:1140-44.
- 10) Buxton R & Frank L. A Model for the Coupling Between Cerebral Blood Flow and Oxygen Metabolism During Neural Stimulation. *J Cereb Blood Flow Metab* 1997; 17: 64-72.
- 11) Attwell D, Buchan AM, Charpak S, Lauritzen M, Macvivar BA, Newman EA. Glial and neuronal control of brain blood flow. *Nature* 2011; 468(7321): 232-43
- 12) Wang D, Chen Y, Fernandez-Seara M, Detre J. Potentials and challenges for arterial spin labelling in pharmacological magnetic resonance imaging. *J Pharmacol Exp Ther* 2011; 337: 359-66.

13) Maleki N, Brawn J, Barmettler G, Borsook D, Becerra L. Pain response measured with arterial spin labeling. *NMR Biomed* 2013; 26: 664-73.

14) Floyd TF, Ratcliffe SJ, Wang J, Resch B, Detre JA. Precision of the CASL-perfusion MRI technique for the measurement of cerebral blood flow in whole brain and vascular territories. *J Magn Reson Imaging* 2003; 18: 649-55.

15) Hermes M, Hagemann D, Britz P, Lieser S, Rock K, Naumann E, Walter C. Reproducibility of continuous arterial spin labeling perfusion MRI after 7 weeks. *MAGMA* 2007; 20:103-15.

16) Chen Y, Wang D, Detre J. Test-retest reliability of arterial spin labeling with common labeling strategies. *J Magn Reson Imaging* 2011; 33: 940-49.

17) Gevers S, van Osch MJ, Bokkers RP, Kies DA, Teeuwisse WM, Majoie CB *et al.* Intra- and multicenter reproducibility of pulsed, continuous and pseudo-continuous arterial spin labeling methods for measuring cerebral perfusion. *J Cereb Blood Flow Metab* 2011; 31:1706-15.

18) Wu WC, Jiang SF, Yang SC, Lien SH. Pseudocontinuous arterial spin labeling perfusion magnetic resonance imaging--a normative study of reproducibility in the human brain. *Neuroimage* 2011; 56:1244-50.

19) Jain V, Duda J, Avants B, Giannetta M, Xie SX, Roberts T *et al.* Longitudinal reproducibility and accuracy of pseudo-continuous arterial spin-labeled perfusion MR-imaging in typically developing children. *Radiology* 2012; 263: 527-36.

20) MacIntosh BJ, Filippini N, Chappell MA, Woolrich MW, Mackay CE, Jezzard P. Assessment of arterial arrival times derived from multiple inversion time pulsed arterial spin labeling MRI. *Magn Reson Med* 2010; 63: 641-7.

21) Bokkers RP, Bremmer JP, van Berckel BN, Lammertsma AA, Hendrikse J, Pluim JP *et al.* Arterial spin labeling perfusion MRI at multiple delay times: a correlative study with H(2)(15)O positron emission tomography in patients with symptomatic carotid artery occlusion. *J Cereb Blood Flow Metab* 2010; 30(1): 222-9.

22) Wu B, Lou X, Wu X, Ma L. Intra- and interscanner reliability and reproducibility of 3D whole-brain pseudo-continuous arterial spin-labeling MR perfusion at 3T. *J Magn Reson Imaging* 2014; 39(2): 402-9

23) Wang D, Alger J, Qiao J, Gunther M, Pope W, Saver J *et al.* Multi-delay multi-parametric arterial spin-labeled perfusion MRI in acute ischemic stroke – Comparison with dynamic susceptibility contrast enhanced perfusion imaging. *Neuroimage Clin* 2013; 3: 1-7.

24) Chappell MA, MacIntosh BJ, Donahue MJ, Gunther M, Jezzard P, Woolrich MW.

1
2
3 Separation of macrovascular signal in multi-inversion time arterial spin labelling MRI.
4 *Magn Reson Med* 2010; 63: 1357-65.

5
6
7 25) Parkes L, Rashid W, Chard D, Tofts P. Normal cerebral perfusion measurements
8 using arterial spin labeling: reproducibility, stability, and age and gender effects. *Magn*
9 *Reson Med* 2004; 51: 736-43.

10
11 26) Kim D, Adalsteinsson E, Glover G, Spielman D. Regularized higher-order in vivo
12 shimming. *Magn Reson Med* 2002; 48: 715-22.

13
14 27) Okell T, Chappell M, Kelly M, Jezzard P. Cerebral Blood Flow Quantification using
15 Vessel-Encoded Arterial Spin Labeling. *J Cereb Blood Flow Metab* 2013; 33: 1716-
16 1724.

17
18 28) Aslan S, Xu F, Wang PL, Uh J, Yezhuvath US, van Osch M, Lu H. Estimation of
19 labeling efficiency in pseudocontinuous arterial spin labeling. *Magn Reson Med* 2010;
20 63: 765-71.

21
22 29) Smith S. Fast robust automated brain extraction. *Hum Brain Mapp* 2002; 17:143-55.

23
24 30) Jenkinson M, Bannister P, Brady M, Smith S. Improved optimization for the robust
25 and accurate linear registration and motion correction of brain images. *Neuroimage*
26 2002; 17: 825-41.

27
28 31) Chappell MA, Groves AR, Whitcher B, Woolrich MW. Variational Bayesian inference
29 for a non-linear forward model. *IEEE Transactions on Signal Processing* 2009; 57: 223-
30 36.

31
32 32) Greve D & Fischl B. Accurate and robust brain image alignment using boundary-
33 based registration. *Neuroimage* 2009; 48: 63-72.

34
35 33) Andersson J, Jenkinson M, Smith S. Non-linear registration, aka Spatial
36 normalisation: *FMRIB technical report TR07JA2* 2007. FMRIB Analysis Group of the
37 University of Oxford.

38
39 34) Zhang Y, Brady M, Smith S. Segmentation of brain MR images through a hidden
40 Markov random field model and the expectation-maximization algorithm. *IEEE Trans*
41 *Med Imaging* 2001; 20: 45-57.

42
43 35) Bland J & Altman D. Measurement error proportional to the mean. *BMJ* 1996; 313:
44 106.

45
46 36) Shrout P & Fleiss J. Intraclass correlations: uses in assessing rater reliability.
47 *Psychol Bull* 1979; 86: 420-28.

48
49 37) Fleiss J, Levin B, Paik M. *Statistical Methods for Rates and Proportions*. John Wiley
50 & Sons, 2003.

38) Portas CM, Rees G, Howsemann AM, Josephs O, Turner R, Frith CD. A Specific Role for the Thalamus in Mediating the Interaction of Attention and Arousal in Humans. *J Neurosci* 1998; 18: 8979-89.

39) Xie J, Clare S, Gallichan D, Gunn R, Jeppard P. Real-time adaptive sequential design for optimal acquisition of arterial spin labeling MRI data. *Magn Reson Med* 2008; 64: 203-10.

40) Petersen E, Mouridsen K, Golay X. The QUASAR reproducibility study, Part II: Results from a multi-center Arterial Spin Labelling test-retest study. *Neuroimage* 2010; 49: 104-13.

TABLES

Table 1

CBF wsCV (%)

ROI	Session repeat	Week repeat	Month repeat	All sessions (Intra-subject)
GM	3.32	5.33	9.95	6.44
WM	5.36	6.29	11.73	8.27
Frontal lobe	3.58	5.34	9.27	6.69
Temporal lobe	4.82	7.16	11.10	6.88
Parietal lobe	2.53	3.83	8.94	6.42
Occipital lobe	6.79	11.09	13.46	10.43
Insular cortex	7.17	8.04	12.99	8.37
Thalamus	9.20	12.88	13.53	10.92
Caudate	5.98	9.64	12.76	9.55
Putamen	4.34	6.96	9.51	7.25

CBF Intraclass correlation

ROI	Session repeat	Week repeat	Month repeat	All sessions
GM	0.914	0.711	0.181	0.472
WM	0.668	0.235	*	*
Frontal lobe	0.894	0.8	0.516	0.655
Temporal lobe	0.864	0.682	0.087	0.462
Parietal lobe	0.936	0.875	0.598	0.716
Occipital lobe	0.847	0.403	0.446	0.477
Insular cortex	0.67	0.623	0.062	0.393
Thalamus	0.75	0.481	0.557	0.632
Caudate	0.821	0.834	0.5	0.684
Putamen	0.846	0.811	0.403	0.556

CBF reproducibility measures for key ROIs across repeat sessions. **Top)** Lower within subject coefficient of variation (wsCV) values reflect better reproducibility, values < 20% are considered to be in the normal range for ASL data (Gevers et al. 2011). **Bottom)** Interclass correlation coefficient (ICC) values range from 0-1. We designated ICC values <0.4 as poor; 0.4-0.59 as fair; 0.6-0.74 as good; and >0.75 as excellent (Fleiss et al. 2003). * out of range

Table 2

AAT wsCV (%)				
ROI	Session repeat	Week repeat	Month repeat	All sessions (Intra-subject)
GM	1.36	3.25	2.13	2.20
WM	2.73	1.06	2.24	1.69
Frontal lobe	1.79	4.36	3.01	2.94
Temporal lobe	1.97	2.35	2.06	1.79
Parietal lobe	1.37	3.42	2.50	2.28
Occipital lobe	1.70	3.11	2.48	2.20
Insular cortex	2.37	3.54	3.73	3.11
Thalamus	4.54	4.34	3.67	2.76
Caudate	2.12	3.94	6.27	4.25
Putamen	2.91	4.12	2.51	2.93

AAT Intraclass correlation				
ROI	Session repeat	Week repeat	Month repeat	All sessions
GM	0.908	0.526	0.689	0.652
WM	*	0.23	*	0.016
Frontal lobe	0.84	0.243	0.483	0.443
Temporal lobe	0.652	*	0.47	0.262
Parietal lobe	0.875	0.673	0.654	0.732
Occipital lobe	0.885	0.49	0.524	0.61
Insular cortex	0.534	0.185	0.121	0.088
Thalamus	0.597	0.496	0.722	0.667
Caudate	0.812	0.745	0.829	0.795
Putamen	0.757	0.713	0.643	0.551

AAT reproducibility measures for key ROIs across repeat sessions. **Top)** Lower within subject coefficient of variation (wsCV) values reflect better reproducibility, values < 20% are considered to be in the normal range for ASL data (Gevers et al. 2011). **Bottom)** Interclass correlation coefficient (ICC) values range from 0-1. We designated ICC values <0.4 as poor; 0.4-0.59 as fair; 0.6-0.74 as good; and >0.75 as excellent (Fleiss et al. 2003). * out of range

Table 3

Mean Δ CBF increase / %			Within session		
ROI	Run 1	%	Run 2	%	
V1	14.64	34	14.46	34	
Functional V1	17.58	43	17.34	43	
Functional M1 (left)	16.30	38	13.17	28	
Functional M1 (right)	13.51	36	13.29	32	

Mean Δ CBF increase / %			Across session			
ROI	Session 1	%	Session 2	%	Session 3	%
V1	15.22	34	14.54	35	12.60	31
Functional V1	18.41	43	17.99	45	15.63	40
Functional M1 (left)	14.08	33	17.07	40	18.08	45
Functional M1 (right)	13.37	33	14.84	41	14.85	41

Reproducibility of activation within key ROIs during the visual-cued motor task paradigm. Within session (n=6) and across session (n=7) comparisons are displayed for group mean absolute CBF and mean percentage changes between ON and OFF blocks (ON - OFF). Absolute CBF was extracted from both anatomical and functional ROI masks for the visual and motor cortices.

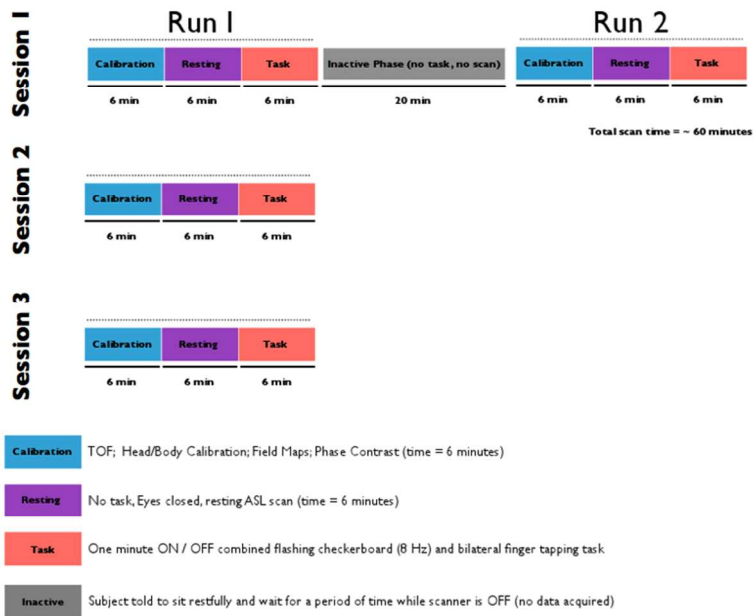
TITLES AND LEGENDS TO FIGURES

Figure 1: A schematic of the experimental design used. Session 1 consisted of two repeat runs of the experimental scans. Runs 1 and 2 were separated by an inactive rest block. Session 2 was completed one week later. Session 3 was completed one month later.

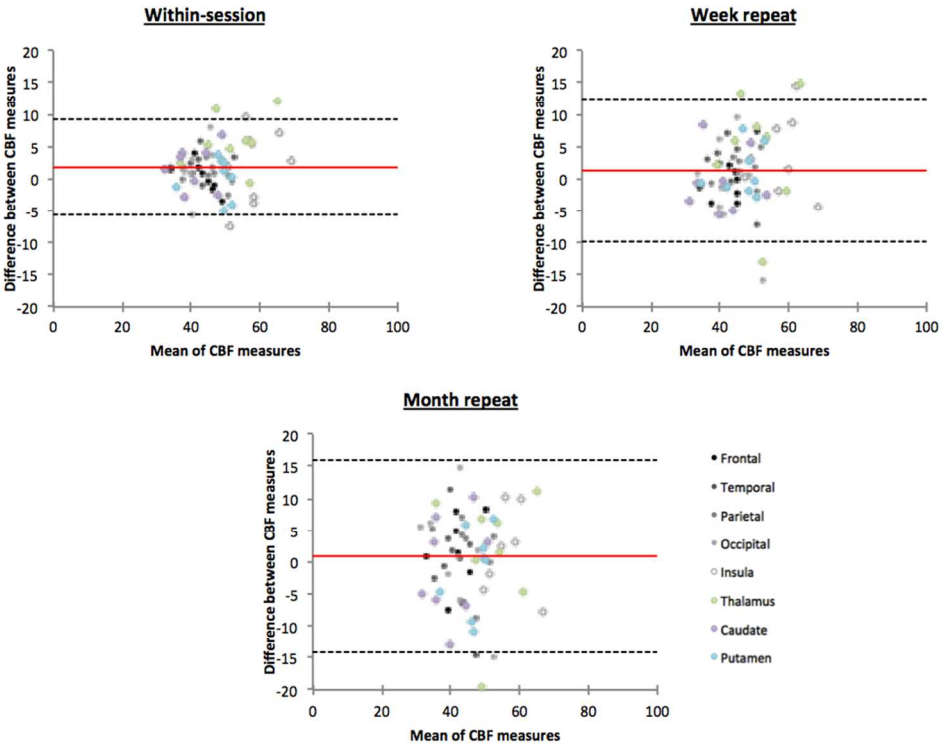
Figure 2: Bland-Altman plots showing repeatability of the absolute CBF measures (ml blood/ 100 g tissue / 1 minute). The red line denotes the bias from 0, the top and bottom lines in black denote the 95% confidence intervals (bias $\pm 1.96 \times \text{SD}$). The difference between measures is always the first session minus the second session. Data shown represents the absolute CBF values from 8 representative brain regions for all 8 subjects.

Figure 3: Hyperperfusion during visual-cued motor task. Statistical maps represent voxels with suprathreshold activation across the group during the task ON versus OFF blocks (Mixed Effects; $z > 2.3$, $p < 0.05$: cluster corrected). A repeated-measures ANOVA revealed no significant differences in hyperperfusion (or hypoperfusion) maps across repeat sessions. Each row represents group mean statistics maps for a given scan session (1-3 and all sessions combined). The whole brain volume is divided into axial slices (z : 10-70) with a single image taken every 5 slices. Images are in radiological convention.

Figure 4: Optimization of TI selection based on cortical region location. PLD values: A 0.25, B 0.5, C 0.75, D 1, E 1.25, F 1.5. Here, extent of ASL signal optimization is assessed for each PLD. The optimization metric (γ) is generated by calculation of the relationship between AAT, PLD and the slice being imaged at a particular time (Equation 1). To note, a given PLD defines the time at which the first, most inferior lying slice is acquired. Subsequently slices are acquired in sequential ascending order at a time $t = \text{PLD} + (z * \text{slice dt})$; where z = the slice number and “slice dt” is the acquisition time for a single slice. Briefly, colour coding details the extent of optimization for each PLD across the whole brain where the darker the colour, the greater the SNR benefit of a given TI (in the context of a single-TI study) at a given brain region (i.e. the closer γ tends to zero). Blue indicates good CBF estimation, although a brighter blue indicates reduced SNR benefit. The whole brain volume is divided into axial slices ($z=10-70$) at 5-slice intervals. All images are in radiological convention.



A schematic of the experimental design used. Session 1 consisted of two repeat runs of the experimental scans. Runs 1 and 2 were separated by an inactive rest block. Session 2 was completed one week later. Session 3 was completed one month later.
86x65mm (300 x 300 DPI)

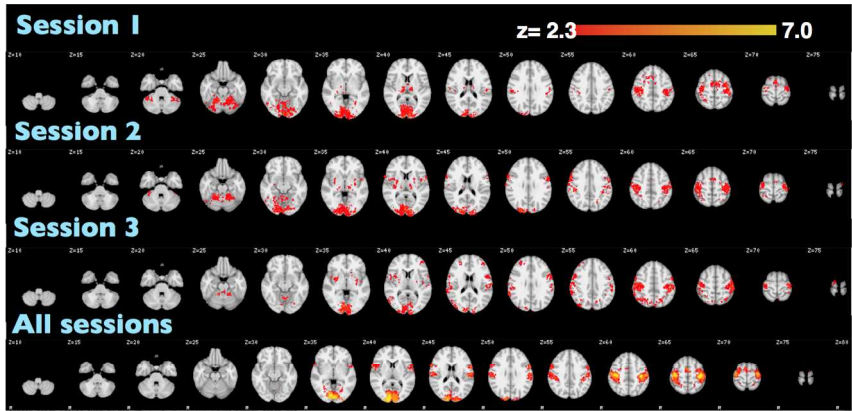


Bland-Altman plots showing repeatability of the absolute CBF measures (ml blood/ 100 g tissue / 1 minute). The red line denotes the bias from 0, the top and bottom lines in black denote the 95% confidence intervals (bias $\pm 1.96 \times \text{SD}$). The difference between measures is always the first session minus the second session. Data shown represents the absolute CBF values from 8 representative brain regions for all 8 subjects.

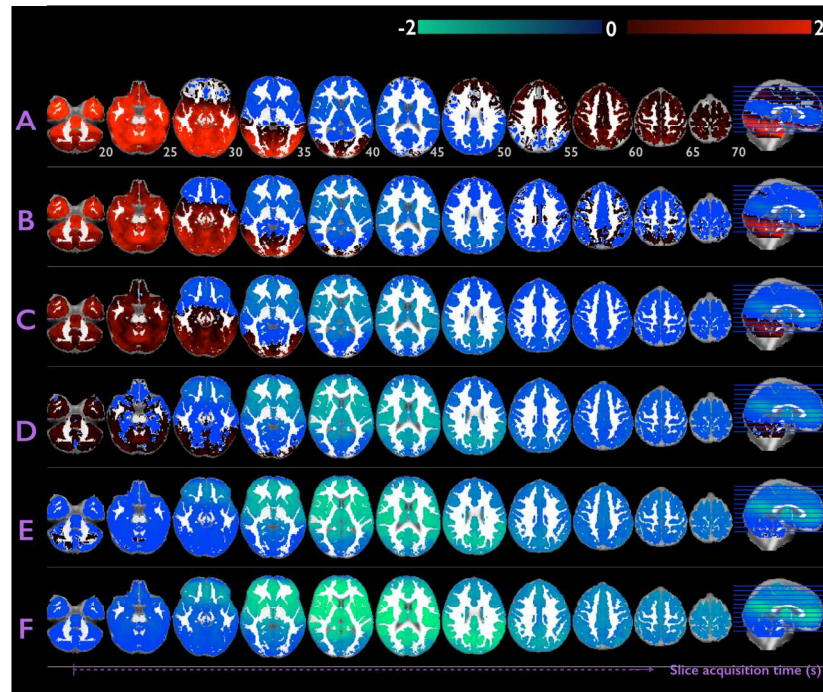
361x270mm (72 x 72 DPI)

Visual-cued motor task activation

Mixed Effects; $z > 2.3$, $p < 0.05$
(cluster corrected)



Hyperperfusion during visual-cued motor task. Statistical maps represent voxels with suprathreshold activation across the group during the task ON versus OFF blocks (Mixed Effects; $z > 2.3$, $p < 0.05$: cluster corrected). A repeated-measures ANOVA revealed no significant differences in hyperperfusion (or hypoperfusion) maps across repeat sessions. Each row represents group mean statistics maps for a given scan session (1-3 and all sessions combined). The whole brain volume is divided into axial slices (z : 10-70) with a single image taken every 5 slices. Images are in radiological convention.
529x740mm (72 x 72 DPI)



Optimisation of TI selection based on cortical region location. PLD values: A 0.25, B 0.5, C 0.75, D 1, E 1.25, F 1.5. Here, extent of ASL signal optimisation is assessed for each PLD. The optimisation metric (γ) is generated by calculation of the relationship between AAT, PLD and the slice being imaged at a particular time (Equation 1). To note, a given PLD defines the time at which the first, most inferior lying slice is acquired. Subsequently slices are acquired in sequential ascending order at a time $t = \text{PLD} + (z * \text{slice dt})$; where z = the slice number and "slice dt" is the acquisition time for a single slice. Briefly, colour coding details the extent of optimisation for each PLD across the whole brain where the darker the colour, the greater the SNR benefit of a given TI (in the context of a single-TI study) at a given brain region (i.e. the closer γ tends to zero). Blue indicates good CBF estimation, although a brighter blue indicates reduced SNR benefit. The whole brain volume is divided into axial slices ($z=10 - 70$) at 5-slice intervals. All images are in radiological convention.

529x740mm (72 x 72 DPI)

1
2
3
4
5
6
7
8
9
10
11
12
13
14
15
16
17
18
19
20
21
22
23
24
25
26
27
28
29
30
31
32
33
34
35
36
37
38
39
40
41
42
43
44
45
46
47
48
49
50
51
52
53
54
55
56
57
58
59
60

Confidential: For Review Only